



ELSEVIER

Available online at [www.sciencedirect.com](http://www.sciencedirect.com)

Physica B ■ (■■■■) ■■■-■■■

PHYSICA B

[www.elsevier.com/locate/physb](http://www.elsevier.com/locate/physb)

# Anisotropy energy distribution determined by mössbauer spectroscopy in a metallic glass

F.H. Sánchez<sup>a,\*</sup>, E.C. Passamani<sup>b</sup>, P. Mendoza Zélis<sup>a</sup>, A. Biondo<sup>b</sup>, M. Vázquez<sup>c</sup>,  
J.R. Proveti<sup>b</sup>, C. Larica<sup>b</sup>, A.F. Cabrera<sup>a</sup>, E. Baggio Saitovitch<sup>d</sup>

<sup>a</sup>Departamento de Física-FCE, Universidad Nacional de La Plata, Casilla de Correos 67 (1900), La Plata, Argentina

<sup>b</sup>Departamento de Física-CCE, Universidade Federal do Espírito Santo, (29060-900), Es, Vitória, Brazil

<sup>c</sup>Instituto de Ciencia de Materiales, CSIC. 28049 Madrid, Spain

<sup>d</sup>Centro Brasileiro de Pesquisas Físicas, (22290-180), RJ, Brazil

## Abstract

The distribution of frozen-in magnetic anisotropy in as-quenched Fe<sub>73.5</sub>Si<sub>13.5</sub>Cu<sub>1</sub>Nb<sub>3</sub>B<sub>9</sub> amorphous melt-spun ribbons was studied by Mössbauer effect spectroscopy, using the temperature-dependent magnetoelastic effect produced on the metallic glass by 1 μm Al coatings. Al coatings were deposited by RF sputtering at  $T \approx 350$  K on both sides of the amorphous ribbons. Estimated magnetic anisotropy values were below 1 kJ/m<sup>3</sup>, with preeminence of anisotropy energy densities lower than 300 J/m<sup>3</sup>.

© 2006 Published by Elsevier B.V.

**Keywords:** Amorphous ribbons; Magnetoelastic effects; Mössbauer spectroscopy; Sensor devices

## 1. Introduction

Intrinsic stresses determine the domain structure in amorphous metal melt-spun ribbons. The application of external stresses also induces magnetoelastic anisotropy and modifies the domain structure. For example, tensile stresses favor a longitudinal magnetization easy axis [1] (for positive magnetostriction). Magnetoelastic effects have been currently used in several magnetoelastic sensor devices. Recently, sensing devices have been proposed where melt-spun amorphous ribbons are glued on one or both sides with materials of different nature. The components exhibiting different thermal expansion coefficients make these composite multilayers good candidates for temperature sensors [2–4]. In these devices, sensing is performed through permeability, which is modified by the stress. Consequently, in-depth knowledge about mechanical stresses in those materials is also of interest for practical reasons. In most of these prototypes, 20 μm-thick melt-spun amorphous ribbons and different metallic coatings with thickness between a few micrometers and several

tens of micrometers, stuck to the ribbons by means of a special glue, were used.

In this paper, it will be shown that Mössbauer effect (ME) spectroscopy offers the possibility of obtaining information on the magnetoelastic effects created by melt-spinning processing and other sources of stresses (e.g., those generated by glued in the above-mentioned sensor devices). ME spectroscopy presents the advantage of sampling the distribution of magnetization direction within the sample bulk as well as in the surface neighborhoods. The mapping is performed easily by evaluating the relative intensities of absorption lines [5]. This methodology averages the information over the whole material, therefore providing only the mean value of the magnetization direction. However, as essentially just domains that follow either an easy axis parallel to the ribbons' surface or perpendicular to it have been observed in these melt-spun materials [6], the amount of in-plane and out-of-plane magnetic moment can be readily estimated.

The objective of this work is to present original results about the distribution of bulk anisotropies induced by the stresses frozen-in during the ribbons fabrication, as well as

\*Corresponding author. Tel.: +54 221 4246062; fax: +54 221 4252006.

E-mail address: [sanchez@fisica.unlp.edu.ar](mailto:sanchez@fisica.unlp.edu.ar) (F.H. Sánchez).

1 after sputtering films of Al on both sides of an amorphous  
ribbon.

## 2. Experimental

20 Twenty micron thick amorphous  $\text{Fe}_{73.5}\text{Si}_{13.5}\text{Cu}_1\text{Nb}_3\text{B}_9$   
21 alloy ribbons were prepared by the melt-spinning techni-  
22 que. Pieces of ribbons were coated on both sides with  $1\ \mu\text{m}$ -  
23 thick Al layers by RF sputtering at a temperature of  
24 approximately 350 K; we will label these samples as *AaA*  
25 (Al/amorphous/Al) trilayers.

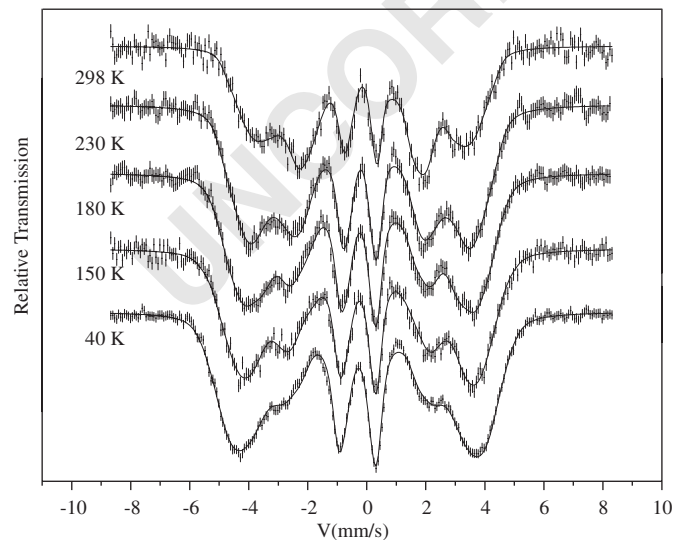
26 Mössbauer experiments were carried out with a standard  
27 constant acceleration spectrometer, under transmission  
28 geometry, using a  $^{57}\text{CoRh}$  source of about 20 mCi.

## 3. Experimental results and discussion

29 Fig. 1 shows some of the Mössbauer spectra obtained  
30 from the *AaA* sample at different temperatures. The  
31 patterns of six broad absorption lines are the typical ones  
32 observed for magnetic metallic glasses. The mean orienta-  
33 tion of Fe magnetic moments can be calculated from the  
34 Mössbauer spectrum using the well-known expression for  
35 the absorption line relative intensities  $3:z:1:1:z:3$ , where  
36  $z = 4 \sin^2(\theta)/(1 + \cos^2(\theta))$ ,  $\theta$  being the angle between the  
37 incident  $\gamma$ -ray and the direction of the magnetization [5].  
38 The incident photon direction was along the normal to the  
39 ribbon surface. As shown in Fig. 1, the relative intensities  
40 of the absorption lines change with temperature.

41 The temperature dependence of the intensity ratio of  
42 lines 2–3,  $I_{23} = z$  can be better observed in Fig. 2 for coated  
43 and uncoated amorphous ribbons. While  $I_{23}$  strongly  
44 depends on temperature for the *AaA* sample, within  
45 experimental error it remains constant for pure amorphous  
46 ribbons.

47 For the trilayers used in this work, important tensile or  
48 compressive stress appears on the individual layers when



57 Fig. 1. ME spectra of *AaA* sample obtained at different temperatures.

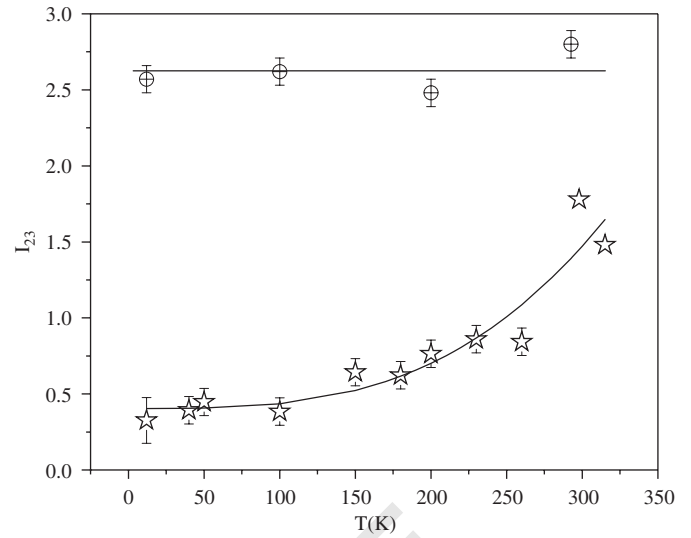


Fig. 2. Temperature dependence of  $I_{23}$  for pure amorphous (circles) and *AaA* samples (stars). The full lines are only guide to the eyes.

temperature  $T$  is changed. The effective linear thermal  
expansion coefficient  $\alpha_{\text{eff}}$  of the *AaA* system can be  
estimated from a simple physical model [2].

The strain undergone by the metallic glass for a  
temperature variation  $\Delta T$ , relative to that which would  
occur in the absence of the coating is given by  $\Delta\varepsilon =$   
 $\varepsilon - \varepsilon_{\text{Am}} = (\alpha_{\text{eff}} - \alpha_{\text{Am}}) \Delta T$  and the stress it experiences by  
 $\sigma = E_{\text{Am}} \Delta\varepsilon = E_{\text{Am}} (\alpha_{\text{eff}} - \alpha_{\text{Am}}) \Delta T$ , (1)

where  $\alpha_{\text{Am}}$  ( $\approx 12 \times 10^{-6} \text{ K}^{-1}$ ) and  $E_{\text{Am}}$  ( $\approx 150 \text{ GPa}$ ) are the  
linear thermal expansion coefficient and Young's Modulus  
of the amorphous. In our case, the relative thermal  
expansion coefficient  $\alpha_{\text{eff}} - \alpha_{\text{Am}}$  is about  $5.4 \times 10^{-7} \text{ K}^{-1}$ .

The main energy term affecting magnetization distribu-  
tion is the local bulk anisotropy present in the amorphous  
material induced by the ultra-rapid freezing process. Essen-  
tially two types of domain patterns have been  
observed in melt-spun metallic glasses: wide domains that  
follow a local in-plane easy direction and narrow  
fingerprint-like ones, which follow an easy direction  
perpendicular to the surface [6]. A sketch of this situation  
is given in Fig. 3 which represents one small piece of the  
ribbon submitted to no external stress where regions of  
preferential anisotropy parallel  $K_{\parallel}$  and perpendicular  $K_{\perp}$   
to the surface are indicated. The figure also suggests how new  
out-of-plane magnetization regions would develop when  
temperature is reduced, due to the increase of a compre-  
sive stress generated by the Al layers. In the volume  $V_{\parallel}$   
where  $K \equiv K_{\parallel}$ , volumes  $V_1$  and  $V_2$ , where the local  
anisotropy  $K \geq 3\lambda_S\sigma/2$  and  $K \leq 3\lambda_S\sigma/2$ , can be distin-  
guished. Within  $V_1$  and  $V_2$  the combined effect of stress  
and anisotropy energy contributions leads to magnetiza-  
tion preferential directions given by  $\theta \approx 0$  and  $\theta \approx \pi/2$ ,  
respectively.

Since in  $V_1$ ,  $I_{23} \approx 4$  and in  $V_2$ ,  $I_{23} \approx 0$ , the fraction  $f_j =$   
 $V_j/V$  ( $V$ , total volume) can be estimated by means of the  
expressions

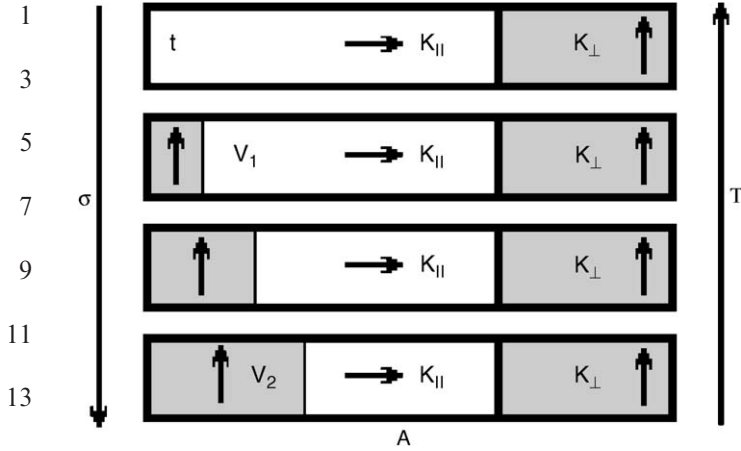


Fig. 3. Regions of ‘quenched’ in-plane and out-of-plane anisotropy,  $K_{||}$  and  $K_{\perp}$ . Small arrows indicate preferential magnetization directions. Large arrows indicate sense of increasing temperature and stress. Gray and white zones do not intend to represent the actual space magnetization distribution.

$$V = V + V_{\perp} = V_1 + V_2 + V_{\perp},$$

$$I_{23} = 4f_1,$$

$$f_2 = 1 - f_1 - f_{\perp} = 1 - f_{\perp} - I_{23}/4.$$

Therefore,  $f_2$  can be estimated experimentally, taken into account that  $f_{\perp}$  can be estimated from the value of  $I_{23}$  obtained from uncoated amorphous ribbon, where  $f_2 = 0$ ,  $f_{\perp} = 1 - I_{23}(\sigma = 0)/4 \approx 0.36$ .

It is possible now to find a relationship between  $f_2$  and the critical value of  $K_{||}$ ,  $K_C = -3\lambda_S\sigma/2$ , by noting that

$$f_2 = \frac{1}{V} \int_{K=0}^{K_C=-3\lambda_S\sigma/2} dV(K_{||}).$$

Fig. 4 is a plot of  $f_2$  vs.  $K_C$  built assuming  $\sigma = 0$  at 350 K; it gives the distribution of  $K_{||}$  within the material. It indicates that frozen in-plane anisotropy is lower than  $1 \text{ kJ/m}^3$ . Furthermore, volume fraction  $f_2$  increases more rapidly for small  $K_C$  values indicating that regions with in-plane anisotropy  $K_C \leq 3 \times 10^2 \text{ J/m}^3$  are more abundant than those with higher  $K_C$  values.

#### 4. Summary and conclusions

It was found that  $1 \mu\text{m}$  Al coatings on both sides of an amorphous melt-spun ribbon produce noticeable changes of the intensity ratio  $I_{23}$  of the ME spectra absorption lines due to the evolution of magnetoelastic effects with temperature. Within the studied temperature range  $dI_{23}/dT$  takes its largest values near RT, being about  $0.001 \text{ K}^{-1}$  at 100 K and  $0.01 \text{ K}^{-1}$  at 293 K. Using a simple model for the distribution of internal stress in pure as-quenched ribbons, the magnitude of the internal stress induced

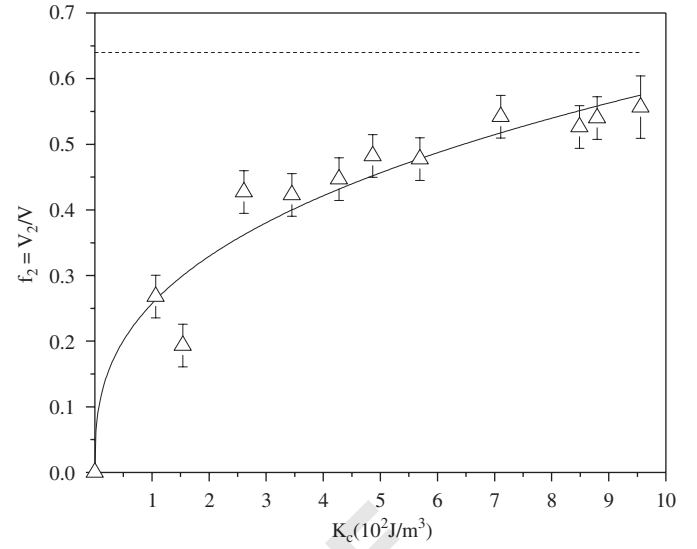


Fig. 4. Empirical estimation of the relationship between the volume fraction where the magnetization is varied from in-plane to out-of-plane by means of the Al-induced compressive stress, and the critical value of in-plane anisotropy for a given stress,  $K_C = -\lambda_S\sigma$  (triangles). The full line is a potential function fit to the data. The dashed line represents the expected upper limit of  $f_2 = 0.64$ .

anisotropy  $K_{||}$  could be estimated, as well as its intensity distribution. As the effect of Al coating increases monotonously with its thickness, it is expected that  $dI_{23}/dT$  values much larger than those presented here can be obtained, thus reducing the temperature interval where main changes take place.

In an on-going work, the study of the effects of different coatings is being extended and deepened, including the investigation of the systems’ response at higher temperatures.

#### Acknowledgments

We acknowledge economic support from CNPq of Brasil, CONICET of Argentina, UFES, UNLP and ICMM.

#### References

- [1] B.D. Cullity, Introduction to Magnetic Materials, Addison-Wesley, Menlo Park, 1972, pp. 266–275.
- [2] Y. Je Bae, H.G. Jang, H.K. Chae, Bull. Korean Chem. Soc. 27 (1996) 621.
- [3] L. Mehnen, H. Pfützner, E. Kaniusas, J. Alloy. Compd. 369 (2004) 202.
- [4] E. Kaniusas, et al., J. Alloy. Compd. 369 (2004) 198.
- [5] A. Vertés, L. Korecz, K. Burger, Mössbauer Spectroscopy, Elsevier Scientific, Budapest, 1979, pp. 13–21.
- [6] A. Hubert, R. Schäfer, Magnetic Domains, Springer, Berlin, 1998, pp. 435–438.

59

61

63

65

67

69

71

73

75

77

79

81

83

85

87

89

91

93

95

97

99

101

103

105

107

109

111

113